

**Supporting Information for**

**Electron capture dissociation of extremely supercharged protein  
ions formed by electrospray ionisation**

Muhammad A. Zenaidee and William A. Donald

## Table of Contents

<b>Title Page</b> .....	1
<b>Table of Contents</b> .....	2
<b>Figure S1.</b> Representative ESI and ECD mass spectra for carbonic anhydrase II.....	3
<b>Figure S2.</b> Representative ESI and ECD mass spectra for bovine serum albumin.....	4
<b>Figure S3.</b> Relative ECD-MS fragment ion abundances for all charge states of cytochrome <i>c</i> 5	
<b>Figure S4.</b> Representative ECD product ion mass spectra for [ubq, 17H] <sup>17+</sup> .....	6
<b>Figure S5.</b> Venn diagram of <i>a</i> , <i>x</i> , and <i>b</i> , <i>y</i> sequence ions for a range of charge states.....	7
<b>Figure S6.</b> Venn diagram of <i>a</i> , <i>x</i> , and <i>b</i> , <i>y</i> sequence ions for a range of proteins.....	8
<b>Figure S7.</b> Theoretical sequence ion abundances vs. mass to correct for isotopic dilution.....	9
<b>Table S1.</b> Effects of cytochrome <i>c</i> concentration on extent of protein ion charging .....	10
<b>Table S2.</b> ECD parameters .....	11
<b>Methods</b> .....	13

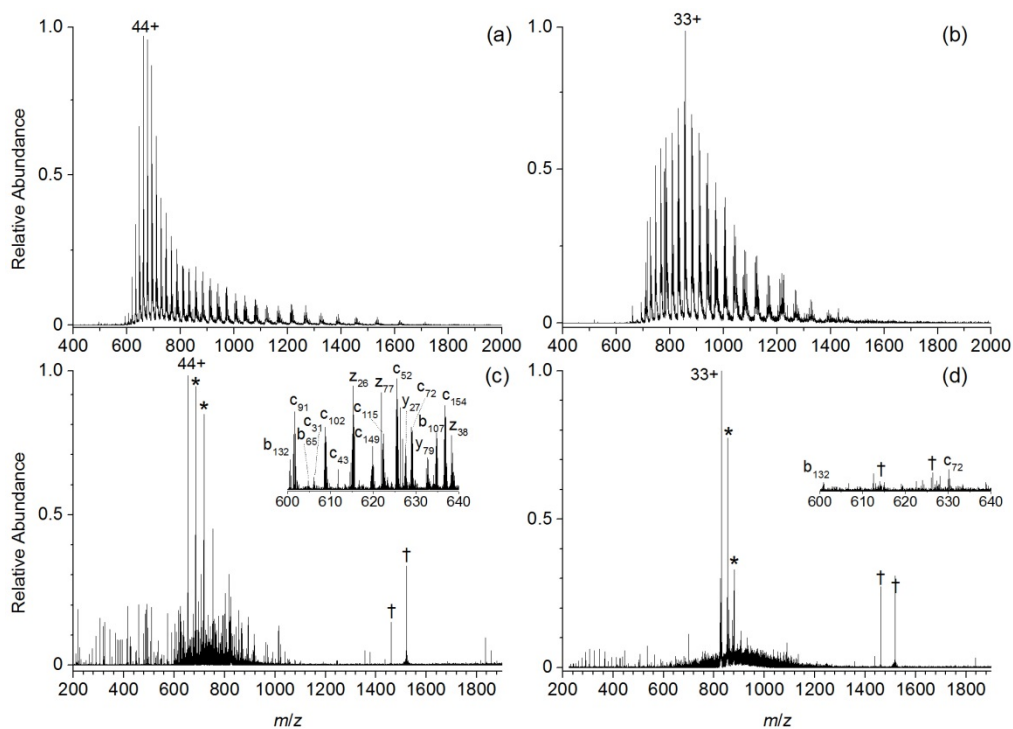


**Figure S1.** ESI mass spectra of aqueous solutions containing 5  $\mu\text{M}$  carbonic anhydrase II, 0.5% acetic acid, and (a) 5% 1,2-butylene carbonate, and (b) no supercharging additive. ECD mass spectra of (c)  $[\text{CAII},44\text{H}]^{44+}$ , and (d)  $[\text{CAII},33\text{H}]^{33+}$ , which were the most abundant charge states formed using each solution. Peaks corresponding to the reduced precursor ions (first and second reductions) and instrumental noise are denoted by “\*” and “†,” respectively.

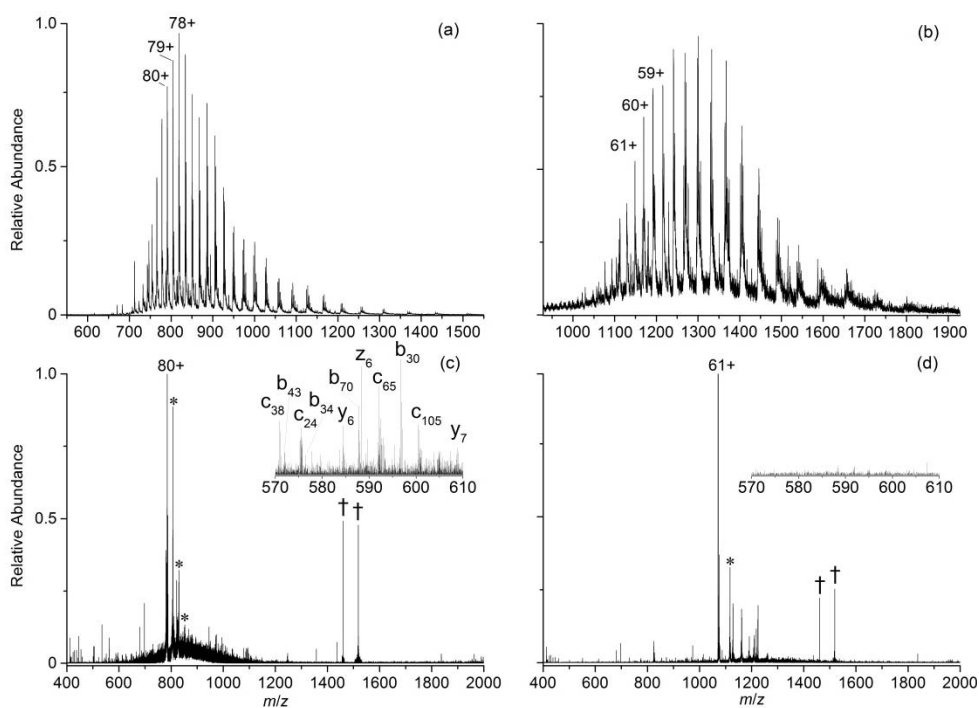


**Figure S2.** ESI mass spectra of aqueous solutions containing 5  $\mu\text{M}$  bovine serum albumin, 0.5% acetic acid, and (a) 5% 1,2-butylene carbonate, and (b) no supercharging additive. ECD mass spectra of (c)  $[\text{BSA},80\text{H}]^{80+}$ , and (d)  $[\text{CAII},61\text{H}]^{61+}$ , which were the most abundant charge states formed using each solution. Peaks corresponding to the reduced precursor ions (first, second, and third reductions) and instrumental noise are denoted by “\*” and “†,” respectively.

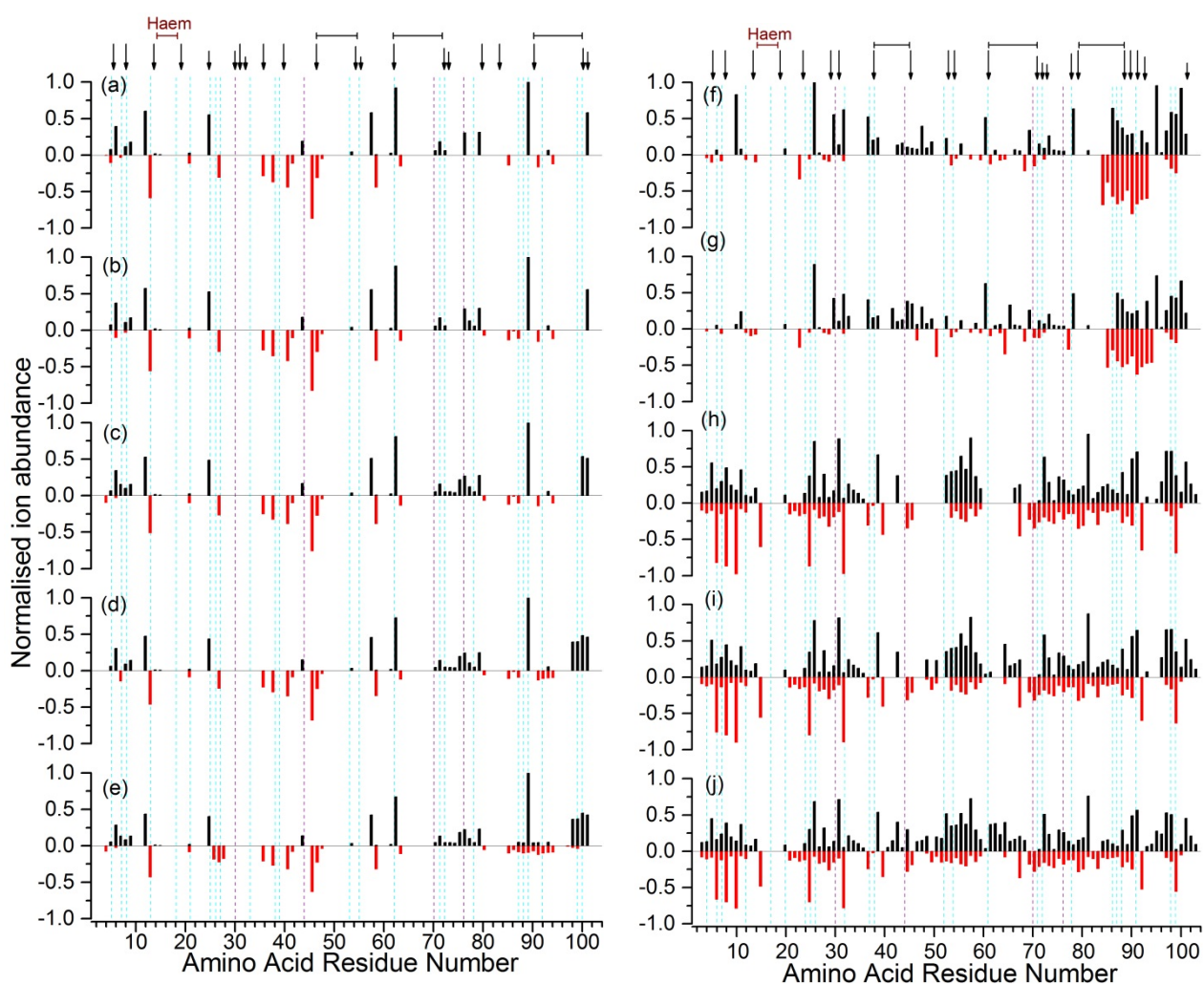


**Figure S3.** Relative ECD-MS fragment ion abundances at each inter-amino acid residue site for isolated (a-e)  $[\text{cyt } c, 15\text{H}]^{15+}$  to  $[\text{cyt } c, 19\text{H}]^{19+}$  and (f-j)  $[\text{cyt } c, 20\text{H}]^{20+}$  to  $[\text{cyt } c, 24\text{H}]^{24+}$ . Protonated protein ions were formed from aqueous solutions containing  $5 \mu\text{M}$  cytochrome *c*, 0.5% acetic acid, and either (a-e) no supercharging additive or (f-j) 5%(v/v) BC. N-terminal and C-terminal fragment ion abundances are positive (black) and negative (red), respectively. Light blue lines indicate positions of basic amino acid residues (Arg, Lys, and His) and purple lines indicate positions of Pro residues. Calculated relative protonation frequencies from reference 13 of the main text are shown as vertical arrows (length proportional to protonation frequency) for protonated *cyt c* [ $16+$ , above panel (a);  $21+$ , above panel (e)]. The

three largest sequences between adjacent amino acid residues that are not predicted to be protonated are shown along with the sequence spanned by the cross-linked haem group.

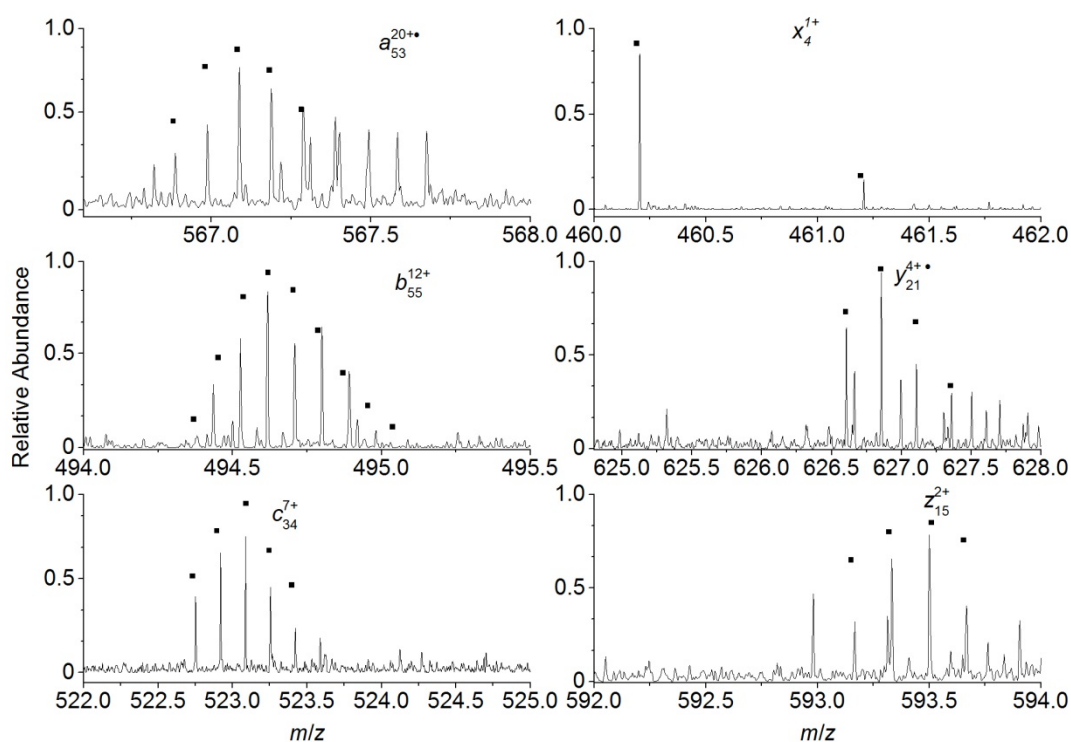


**Figure S4.** Product ion mass spectra of select *a*, *b*, *c*, *x*, *y*, *z* sequence ions formed upon ECD of [ubiquitin,17H]<sup>17+</sup>. Closed squares correspond to the theoretical isotope distributions.

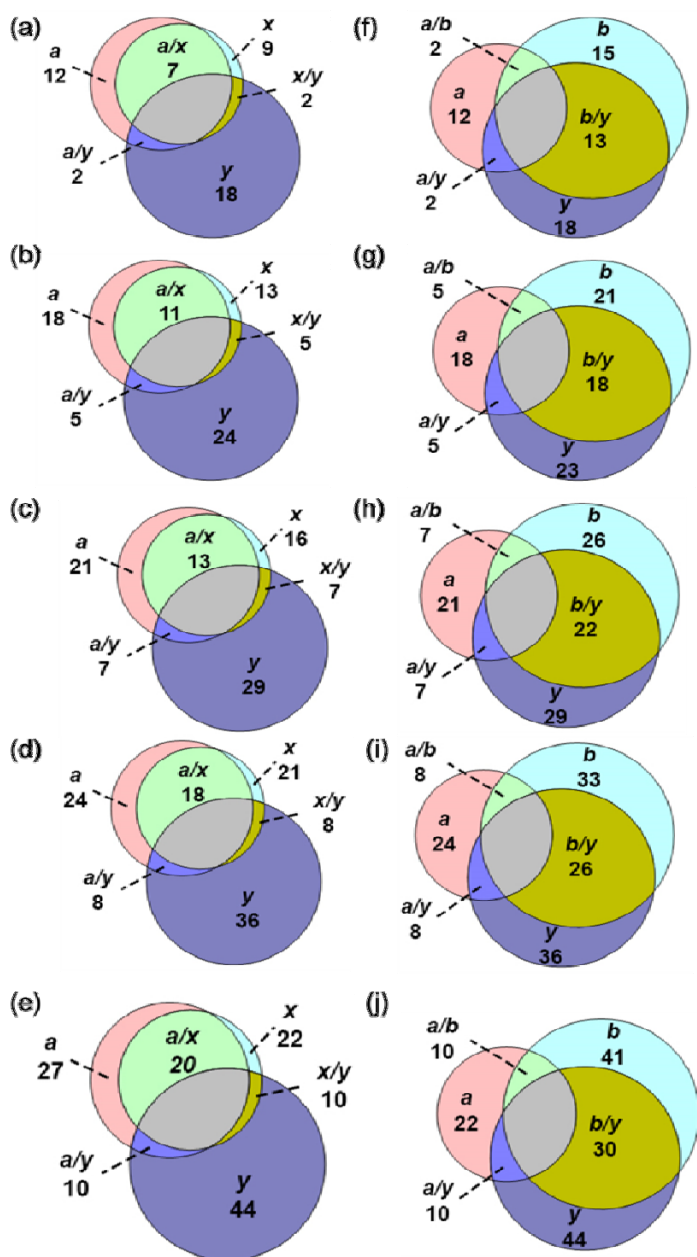


**Figure S5.** Total number of (a-e)  $a$ ,  $x$  and  $y$  sequence ions and (f-j)  $a$ ,  $b$ , and  $y$  sequence ions and total number of sequence ions that correspond to cleavages at common inter-residue sites for protonated cytochrome  $c$  of different charge states, 16+ (a,f), 18+ (b,g), 20+ (c,h), 22+ (d,i), and 24+ (e,j) depicted as Venn diagrams.

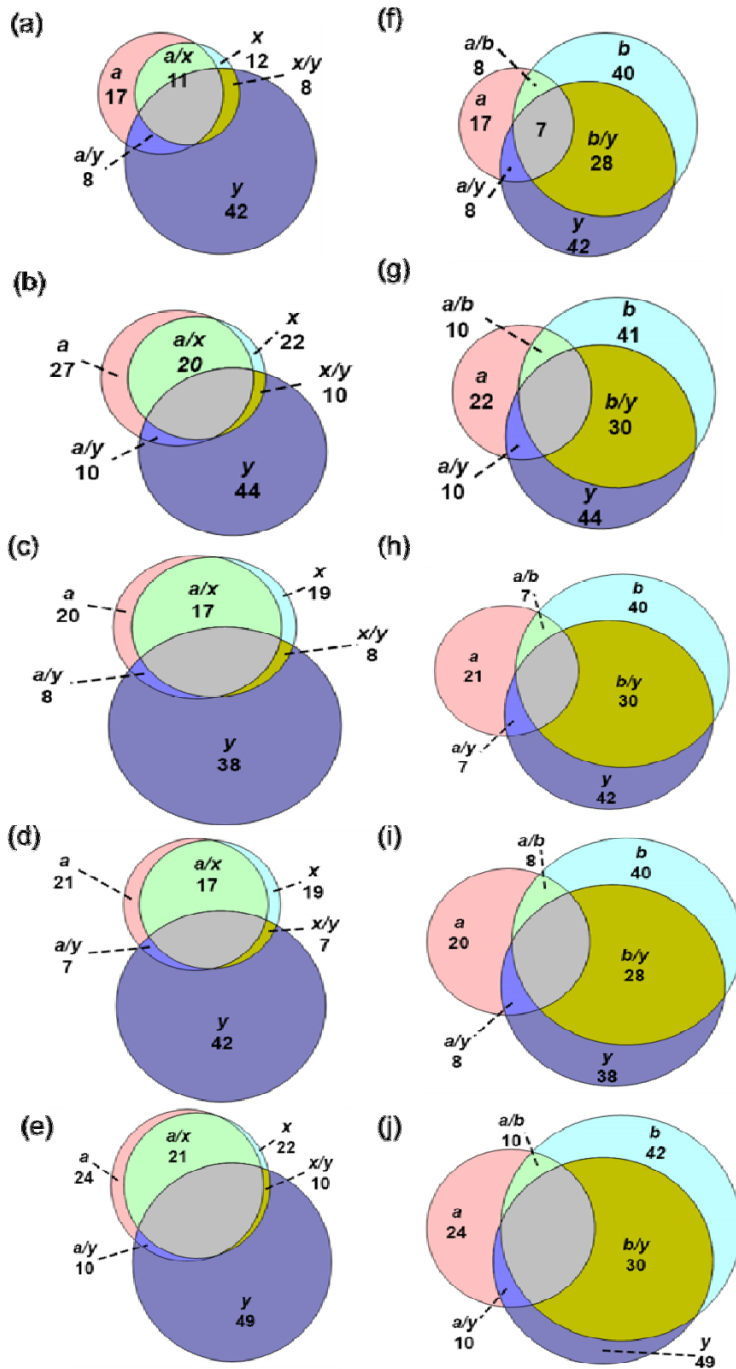


**Figure S6.** Total number of (a-e)  $a$ ,  $x$  and  $y$  sequence ions and (f-j)  $a$ ,  $b$ , and  $y$  sequence ions and the number of sequence ions that correspond to cleavages at common inter-residue sites for the highest charge state of ubiquitin (17+; a,f), cytochrome  $c$  (24+; b,g), haemoglobin (26+; c,h), myoglobin (31+; d,i), and carbonic anhydrase II (44+; e,j), respectively, depicted as Venn diagrams.

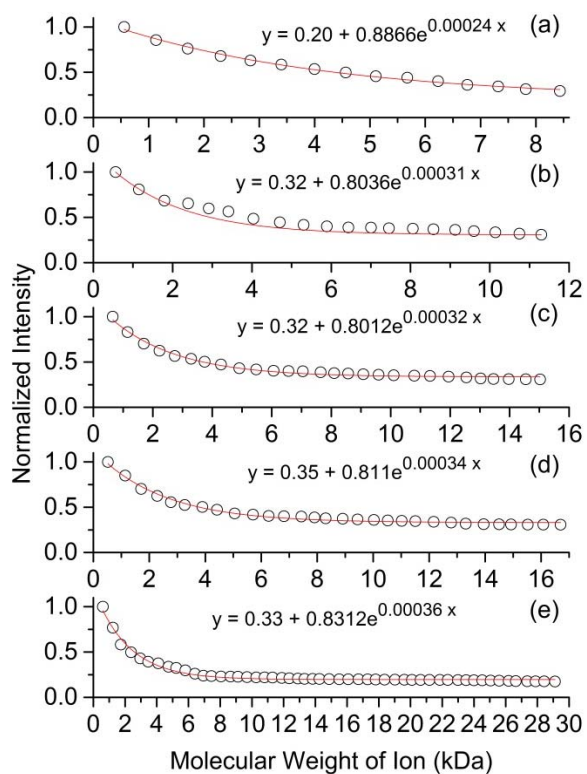


**Figure S7.** Theoretical relative abundance of the most abundant isotopic ion (abundance of most abundant ion normalised by the total abundance of the isotopic distribution) of fragment ions for (a) ubiquitin, (b) cytochrome *c*, (c) haemoglobin, (d) myoglobin and (e) carbonic anhydrase II plotted vs. fragment ion neutral masses. The best fit exponential equations (inset;  $y = y_0 + Ae^{-bx}$ ) were used in order to correct for isotopic dilution in the experimental data (see below).

**Table S1.** The charge state range (highest observed/lowest observed charge state) and average charge state (ACS) of protonated cytochrome *c* ions formed from acidified aqueous solutions containing 5 %(v/v) BC and no BC as a function of cytochrome *c* concentration (5  $\mu$ M to 100  $\mu$ M).

<b>Conc. (<math>\mu</math>M)</b>	<b>Range (+BC)</b>	<b>ACS (+BC)</b>	<b>Range (-BC)</b>	<b>ACS (-BC)</b>
5	25/20	22.7	18/10	15.3
10	25/20	22.6	18/10	15.4
20	25/20	22.5	18/10	15.3
30	25/19	22.3	18/10	15.2
40	25/19	22.4	18/10	15.1
50	25/19	22.5	18/10	15.3
75	24/18	22.4	17/9	15
100	24/18	22.0	17/9	14.9

**Table S2.** The ECD irradiation time, ECD electron energy, and number of scans for each ECD tandem mass spectra.

<b>Protein</b>	<b>Time, ms</b>	<b>Energy, eV</b>
Ubiquitin	25	3.5
Cytochrome <i>c</i>	30	3.3
Haemoglobin	30	3.0
Myoglobin	30	3.0
Carbonic anhydrase II	40	2.5
Bovine serum albumin	50	2.8

## Methods

*Materials.* Bovine ubiquitin (red blood cells; 8.6 kDa), bovine carbonic anhydrase II (erythrocytes; 29 kDa), and equine myoglobin (heart; 17 kDa) were obtained from Sigma-Aldrich. Equine cytochrome *c* (12 kDa), and equine haemoglobin (heart; 16 kDa) were obtained from Alfa Aesar. 1,2 butylene carbonate was obtained from Tokyo Chemical Industries (TCI) and was used without any further purification.

*Analysis.* Sequence ions were assigned by comparing measured  $m/z$  values and isotopic distributions of fragment ions to the theoretical distributions for all possible sequence ions, which were obtained using Protein Prospector (UCSF). The average mass accuracy of the instrument was  $< 1$  ppm. Sequence coverage is defined by the number of unique inter-residue cleavage sites between adjacent amino acids that were identified in the tandem mass spectrum of interest out of the total number of inter-residue sites. The efficiency of electron capture ( $Eff_{\text{ECD}}$ ) was calculated using Eq. S1, where  $\sum I_{\text{F}}$  is the sum of the integrated abundances for each fragment ion, and  $\sum I_{\text{R}}$  and  $I_{\text{P}}$  are the integrated abundances of the reduced precursor ions and isolated precursor ion, respectively.<sup>1</sup> The ECD fragmentation efficiency ( $Eff_{\text{Frag}}$ ) was calculated by Eq. S2.

The difference in  $Eff_{\text{Frag}}$  and  $Eff_{\text{ECD}}$  corresponds to the fraction of the reduced precursor ions that result in bond cleavage, separation of the fragments, and detection of the resulting product ions. Given the large number of fragment ions ( $> 1000$  in total), the abundance of each isotopic cluster was obtained by using the ion abundance of the most abundant ion of

$$Eff_{\text{ECD}} = \frac{\sum I_{\text{F}} + \sum I_{\text{R}}}{\sum I_{\text{F}} + \sum I_{\text{R}} + I_{\text{P}}} \quad (1)$$

$$Eff_{\text{Frag}} = \frac{\sum I_{\text{F}}}{\sum I_{\text{F}} + \sum I_{\text{R}} + I_{\text{P}}} \quad (2)$$

each isotopic cluster. To correct for isotopic dilution, the experimentally measured abundance

of the most abundant ion of each isotopic cluster was normalised by a factor obtained from the best fit equations to plots of the theoretical relative abundance of the most abundant isotope vs mass (Figure S6). Given that ion signal in FT/ICR-MSs increase proportionally with charge state, the ion abundances were divided by the charge state of each ion.

### References

- (1) (a) Zubarev, R. A.; Kelleher, N. L.; McLafferty, F. W., *J. Am. Chem. Soc.* **1998**, *120*, 3265; (b) Iavarone, A. T.; Paech, K.; Williams, E. R., *Anal. Chem.* **2004**, *76*, 2231.